ISSN 1547-4771, Physics of Particles and Nuclei Letters, 2013, Vol. 10, No. 6, pp. 566–572. © Pleiades Publishing, Ltd., 2013.
Original Russian Text © V.M. Bystritsky, E.V. Zubarev, A.V. Krasnoperov, S.Yu. Porohovoi, V.L. Rapatskii, Yu.N. Rogov, A.B. Sadovskii, A.V. Salamatin, R.A. Salmin, V.M. Slepnev, E.I. Andreev, 2013, published in Pis'ma v Zhurnal Fizika Elementarnykh Chastits i Atomnogo Yadra, 2013, No. 6(183), pp. 925–935.

METHODS OF PHYSICAL EXPERIMENT

Gamma Detectors in Explosives and Narcotics Detection Systems

V. M. Bystritsky[a], E. V. Zubarev[a], A. V. Krasnoperov[a], S. Yu. Porohovoi[a], V. L. Rapatskii[a], Yu. N. Rogov[a], A. B. Sadovskii[a], A. V. Salamatin[a], R. A. Salmin[a], V. M. Slepnev[a], and E. I. Andreev[b]

[a]*Joint Institute for Nuclear Research, Dubna, Russia*
[b]*OOO Neutron Technologies, Dubna, Russia*
e-mail: Alexei.Krasnoperov@jinr.ru

Abstract—Gamma detectors based on BGO crystals were designed and developed at the Joint Institute for Nuclear Research. These detectors are used in explosives and narcotics detection systems. Key specifications and design features of the detectors are presented. A software temperature-compensation method that makes it possible to stabilize the gamma detector response and operate the detector in a temperature range from –20 to 50°C is described.

DOI: 10.1134/S154747711306006X

INTRODUCTION

Several experimental systems [1–3] intended for the detection and identification of concealed explosives and narcotics via the tagged neutron method (TNM) were designed and developed at the Joint Institute for Nuclear Research (JINR). The elemental composition of the studied object is determined through the detection of the characteristic gamma radiation that is emitted in the $A(n, n')A$ process of the inelastic scattering of fast neutrons off nuclei of the studied sample. The ING-27 neutron generator [4] serves as the source of neutrons with an energy of 14.1 MeV produced in the $t(d, n)\alpha$ binary reaction.

Let us specify the basic requirements for a detector that registers characteristic gamma radiation. Such a detector needs the following:

(i) high gamma quanta detection efficiency in the energy range of 1–10 MeV;

(ii) low (relative to the γ-quanta detection efficiency) sensitivity to neutron background;

(iii) to be able to provide a linear response;

(iv) high energy and time resolutions in the specified range of γ-quanta energies;

(v) to be radiation-resistant and ensure the temporal stability of its parameters.

The γ-radiation in the energy range specified above is nowadays most frequently detected with the use of detectors based on inorganic scintillators.

1. SCINTILLATORS USED IN TNM SETUPS

A detailed review of the properties of inorganic scintillators that are used for gamma radiation detection in a broad energy range may be found in [5–7]. In the present work, we analyze the properties of scintillators that are used for the detection of explosives and narcotics via the TNM. Basic characteristics of these scintillators are presented in Table 1.

1.1. Sodium Iodide NaI(Tl)

Thallium-activated sodium iodide is the most commonly used scintillator for gamma-radiation detection. It is characterized by high light output, which determines its relative energy resolution (full width at half maximum (FWHM)) of about 7% (if measured for the total absorption peak of gamma quanta with an energy of 662 keV in relatively small crystals).

The high energy and time resolutions, availability, and relatively low cost of γ-detectors based on NaI(Tl) motivated their frequent use in TNM setups, specifically in stationary facilities for bulky cargo inspection [10, 11]. The dependence of the efficiency of detecting gamma quanta with an energy of 4439 keV (determined via the total absorption peak) on the crystal size may be found in [11, 12] (the identification of explosives and narcotics is based on analyzing the characteristic gamma radiation of carbon, nitrogen, and oxygen nuclei with energies of 4439, 5100, and 6130 keV). The efficiency of the gamma-quanta detection of a detector with a ∅5" × 5" NaI(Tl) crystal is 6.5 times higher than the corresponding efficiency of a detector with a ∅3" × 3" crystal. The drawbacks of NaI(Tl) crystals are their hygroscopicity and fragility that limit the use of NaI(Tl) in portable inspection systems. When compared to other scintillators of identical volume from Table 1, NaI(Tl) crystals exhibit the lowest gamma quanta detection efficiency and a higher sensitivity to neutron background.

Table 1. Basic characteristics of scintillators

Properties	Scintillator		
	NaI(Tl)	BGO	$LaBr_3(Ce)$
Density, g/cm^3	3.67	7.13	5.29
Effective atomic number Z	50	75	47
Radiation length, cm	2.59	1.12	1.88
Decay time, ns	245	300	20
Wavelength of maximum emission, nm	410	480	356
Relative light output, %	100	21	130
Refraction index	1.85	2.15	1,9
Melting temperature, °C	651	1050	788
Radiation resistance, Gy	10^3	10^3–10^4	$>3 \times 10^3$ [8]
Hygroscopic	Yes	No	Yes

1.2. Lanthanum Bromide $LaBr_3(Ce)$

The characteristics of γ-detectors based on a lanthanum bromide $LaBr_3(Ce)$ crystal and used in TNM setups were studied in [13, 14]. This crystal exhibits higher light output and better energy resolution (~2.9% at the 662 keV line [13]) than NaI(Tl) crystals. Its short decay time (~20 ns) allows creating γ-detectors that operate at a high event count rate without the substantial deterioration of energy resolution. The time resolution of an α–γ coincidence system (a silicon detector is used for alpha detection, and γ-radiation is registered by a detector based on $LaBr_3(Ce)$) equals ~1.1 ns.

The high cost of $LaBr_3(Ce)$ crystals limits their use. Detectors based on such crystals are, as a rule, installed only in systems with a single detection channel for characteristic γ-radiation [14].

1.3. Bismuth Germanate BGO

The high density and highly effective atomic number of bismuth germanate translate into the fact that BGO-based detectors, when compared to other crystals from Table 1, exhibit the highest gamma-quanta detection efficiency. Table 2 presents the dependence of the efficiency of gamma-quanta detection (determined via the total absorption peak) on their energy for three equally sized crystals.

The time resolution of a BGO crystal equals ~2.1 ns for gamma quanta with an energy of ~1 MeV. Resolution improves with an increase in energy and reaches 890 ps at ~20 MeV [22].

2. γ-DETECTOR DESIGN

An assembled gamma detector is shown in Fig. 1. The BGO crystal [15–17] grown in the Nikolaev Institute of Inorganic Chemistry has the form of a ∅76 × 65 mm cylinder. The scintillation light is detected by the R6233-100 [18] photomultiplier tube (PMT) produced by Hamamatsu Photonics with a gain factor of $\sim 2.3 \times 10^5$ at a supply voltage of ~1000 V. The optical contact between the PMT entrance window and the BGO crystal face is established via an optically transparent epoxy adhesive. The temperature of the crystal is monitored by the TMP36 analog temperature sensor

Table 2. The efficiency of detection of γ-quanta (determined via the total absorption peak) with energies of 0.368, 1.330, and 6.000 MeV in NaI(Tl), $LaBr_3(Ce)$, and BGO crystals relative to the efficiency of detection of γ-quanta with an energy of 1.330 MeV in NaI(Tl) [13]

Crystal	Energy		
	368 keV	1.33 MeV	6 MeV
NaI(Tl) (∅3" × 3")	2.822	1.000	0.259
$LaBr_3(Ce)$ (∅3" × 3")	2.941	1.362	0.457
BGO (∅3" × 3")	3.587	2.514	1.363

Fig. 1. External view of the γ-detector.

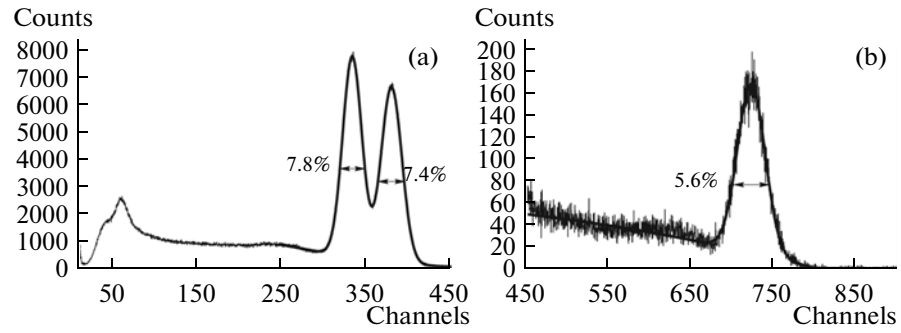

Fig. 2. Amplitude spectrum of γ-quanta from the ^{60}Co isotope. Left panel: peaks of total absorption of γ-quanta with energies of 1173 and 1332 keV. Right panel: peak that corresponds to the simultaneous detection of these quanta with a total energy release of 2505 keV. The line traces the result of fitting the peaks with a Gaussian function under a linear substrate description.

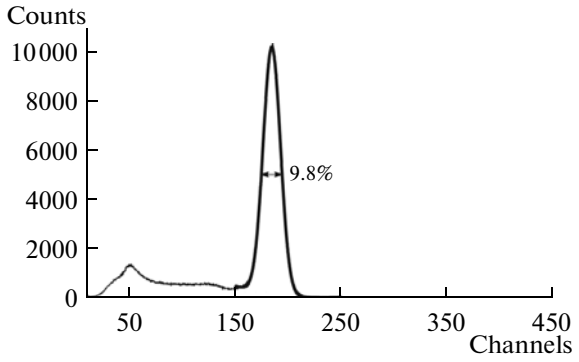

Fig. 3. Amplitude spectrum of γ-quanta from the ^{137}Cs isotope. The line traces the result of fitting the peak of total absorption of γ-quanta with an energy of 662 keV with a Gaussian function under a linear substrate description.

[19]. The PMT with a voltage divider mounted on it is protected with a permalloy shield. The detector is housed within a ∅110 × 260 mm dural case. The mass of the detector equals 3.5 kg.

3. GAMMA-DETECTOR CHARACTERISTICS

The detector response linearity and its energy resolution in the energy range of 0.5–2.6 MeV were determined using the gamma lines of isotopes from the set of standard spectrometric gamma emitters. The widths of total gamma-quanta absorption peaks (see Table 3) and the positions of their maxima in the amplitude spectrum were determined by fitting the peaks with a Gaussian function under a linear background description. The measured dependence of the detector response on the gamma quantum energy is represented by a straight line with an accuracy of no less than 0.4%.

Figure 2 shows the amplitude spectra of events registered by the γ-detector irradiated by γ-photons of ^{60}Co. The response linearity for γ-quanta with energies in excess of 2.6 MeV was checked directly via the energy spectra of gamma quanta produced by the irradiation of pure carbon and melamine $C_3H_6N_3$ (explosives imitator) samples with fast neutrons. The deviation from linearity in the energy range of 2.6–6.1 MeV does not exceed 0.35%.

The typical relative energy resolution of the detector equals 9.8% at the ^{137}Cs line (see Fig. 3) and 7.8 and 7.4% at the ^{60}Co lines (see Fig. 2) with energies of 1173 and 1332 keV, respectively. The dependence of the relative energy resolution on the γ-quanta energy E_γ is shown on Fig. 4. It is described fairly accurately by the following relation:

$$\frac{\mathrm{FWHM}}{E_\gamma} = \frac{A}{\sqrt{E_\gamma}} + B. \quad (1)$$

Table 3. Isotopes and corresponding gamma-quanta energies

Energy	Isotope								
	^{228}Th	^{228}Th	^{137}Cs	^{54}Mn	^{60}Co	^{60}Co	^{40}K	^{60}Co	^{228}Th
E_γ, keV	511	583	662	835	1173	1332	1461	1173 + 1332	2615

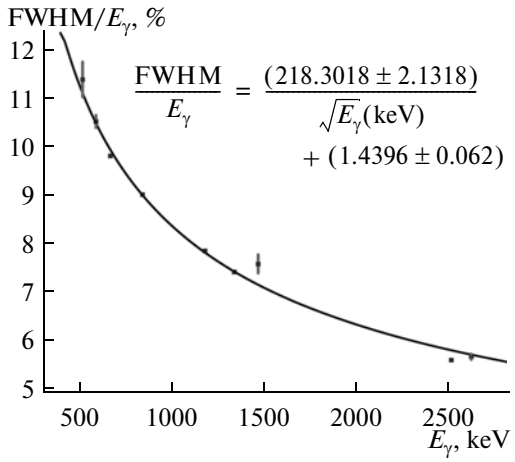

Fig. 4. Dependence of the measured relative energy resolution of the gamma detector on the gamma quanta energy (dots) and the approximation of this dependence by Eq. (1) (line).

The amplitude distribution of events registered by the γ-detector under the irradiation of the ^{12}C sample with fast neutrons is shown in Fig. 5a. The positions and widths of the peaks with energies of 4438 and 3927 keV (the single escape peak corresponding to the escape of a γ-quantum with an energy of 511 keV) were determined by fitting them with a Gaussian function. The γ-detector energy resolution at the 4438 keV line equals 4.6%.

The spectrum of time intervals between the registration of a signal from characteristic γ-quanta of carbon nuclei and the registration of an α signal by the detector from a coincidence system is shown in Fig. 5b. The typical time resolution of the α–γ coincidence system equals 3.2 ns.

4. TEMPERATURE STABILIZATION OF THE γ-DETECTOR

When using γ-detectors based on BGO crystals, one must take into account the fact that the temperature dependence of the light output and decay time of these crystals is rather sharp. If the temperature of the crystal increases from 0 to 40°C, the decay time decreases from 400 to 200 ns and the light output undergoes a more than twofold reduction [6]. The value of the coefficient of light output change depends on the quality of the crystal and falls within interval of 1.0–1.6%/°C.

The energy calibration depending on the light output may be stabilized by thermostating the crystal. This method is used in laboratory measurements and accelerator and reactor experiments with large-scale stationary detection systems. For example, the cooling system [20] of the electromagnetic calorimeter of the L3 experiment carried out at the LEP accelerator (CERN, Geneva) maintained a temperature of more than 11 000 BGO crystals in a range of 17–18°C over the entire period of operation of this facility.

Strict mass and size limitations imposed on portable and mobile inspection systems intended for the detection of explosives and narcotics make it practically impossible to use detector temperature-stabilization devices in such systems. Another approach to the problem of stabilizing the energy calibration of the gamma detection channel lies in correcting the gamma detector amplitude response in accordance with the BGO crystal temperature. An automatic system that compensates for variations in the light output temperature was implemented in the PELAN setup [13]. In order to keep the position of the peak constant, the system varied the detection channel gain ratio in accordance with the BGO crystal temperature changes and the measured temperature dependence of

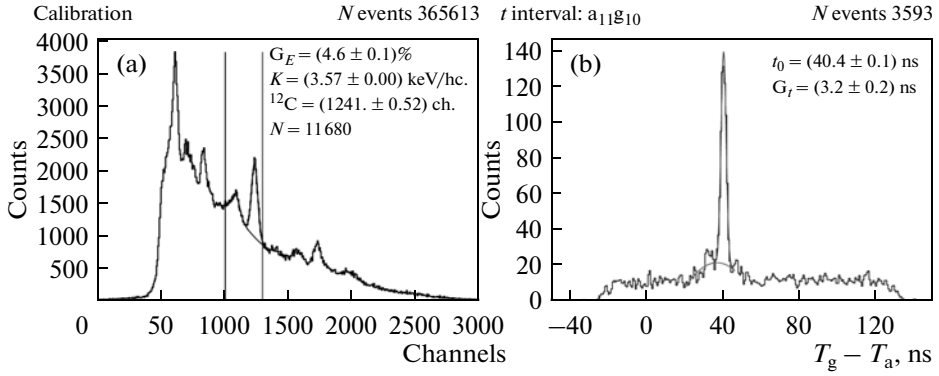

Fig. 5. Left panel: amplitude spectrum of γ-quanta registered by the gamma detector under irradiation of the ^{12}C pure carbon sample with neutrons with an energy of 14.1 MeV. Vertical lines mark out the energy interval of 3927–4438 keV. The positions and widths of the peaks were determined by fitting them with a Gaussian function under quadratic background description. Right panel: spectrum of the time intervals between the moments of registration of signals from the α and γ-detectors in the energy range specified above. The peak corresponds to the signals from gamma quanta coming from the carbon sample that coincide with the signals from the α-detector, while the substrate corresponds to chance coincidences.

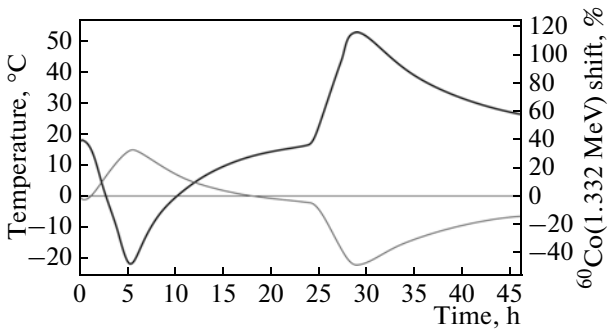

Fig. 6. Variation of the temperature of the crystal (heavy line, scale on the left) and the relative ^{60}Co peak (1.332 MeV) shift (thin line, scale on the right) with time elapsed from the start of the measurements.

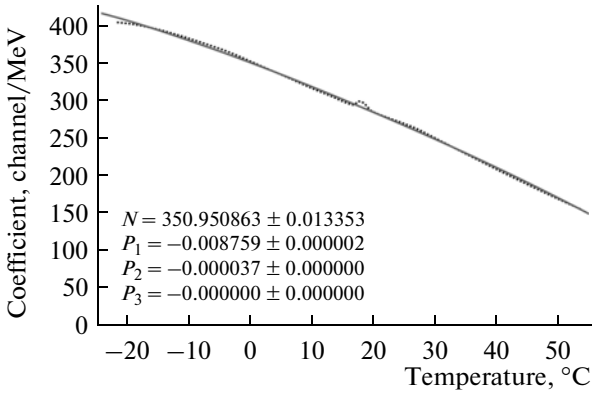

Fig. 7. Measured (dots) and parameterized (line) temperature dependences of the coefficient of conversion of energy into the amplitude spectrum channel number.

its light output [21]. A response-stabilization accuracy of 7% was attained for a BGO temperature varying from −5 to +45°C.

The inspection systems that were designed and developed at the Joint Institute for Nuclear Research utilize the software method of the γ-detector response correction. This method is easily implemented and configured, may be applied to a considerable number of detection channels, and does not require any additional equipment (except for a system to measure the BGO crystal temperature). The γ-detector signal correction is based on measuring the dependence of the response amplitude on the readings of a temperature sensor mounted on the BGO crystal.

This method was applied in the offline processing of data from BGO calorimeters in high-energy particle physics experiments [23, 24]. Our variant of this method is special in that the correction is introduced in real time.

The temperature dependence of the γ-detector response was studied using a climate chamber in the temperature range from −20 to +55°C. The standard ^{137}Cs and ^{60}Co sources served as sources of gamma quanta. The measurements lasted for about 45 h. This time interval was divided into four successive phases: the detector was first cooled to −20°C at a rate of 10°C/h, then warmed up spontaneously and assumed room temperature; then it was heated to +55°C at a rate of 10°C/h and finally cooled spontaneously (see Fig. 6). The temperature of the crystal and the amplitude spectrum of the detector signals were registered by the data acquisition and analysis system with a period of 10 s. Figure 6 shows that cooling the BGO crystal to −20°C resulted in the ^{60}Co peak being shifted from the initial (room-temperature) position by +30%, while heating the crystal to +50°C shifted the peak by 40% towards the low amplitudes side.

The coefficient of conversion of the γ-quantum energy into the amplitude spectrum channel number K_i was determined from the ^{137}Cs and ^{60}Co peaks for each measurement interval i. The dependence of K_i on temperature T_i was described by the following third-order polynomial:

$$F(T) = N\left(1 + \sum_{n=1}^{3} P_n T^n\right), \quad (2)$$

where P_n are the polynomial coefficients and N is the normalizing factor. The polynomial coefficients were determined from the minimization of the following functional:

$$\chi^2 = \sum_{i=1}^{m} \frac{(K_i - F(T_i))^2}{\delta K_i^2 + \delta F_i^2}, \quad (3)$$

where m is the number of measurements, δK_i is the error of determination of the coefficient, and δF_i is the variation of function $F(T)$. This variation depends on the temperature T_i and the error of its measurement δT_i. The $F(T_i)$ describes the K_i measurements with an accuracy of no less than 4%. The deviation rises to maximum in the moments of transition from cooling to heating and vice versa. This may be explained by the inhomogeneity of the temperature distribution in the bulk of the crystal and the fact that the T_i temperature is determined at the edge of the crystal.

The parameterized temperature dependence $F(T)$ of the coefficient of conversion of the gamma quantum energy into the amplitude spectrum channel number is shown on Fig. 7. The $F(T)$ function describes the measured temperature dependence $K(T)$ that is obtained by averaging the K_i values over the temperature range from −0.25 to +0.25°C with an accuracy of no less than 2%.

Normalization of the γ-detector response to the $F(T_0)/F(T)$ ratio, where T is the current measured temperature of the crystal and T_0 is the temperature that specifies the normalization, compensates for the temperature variations of the light output. The correc-

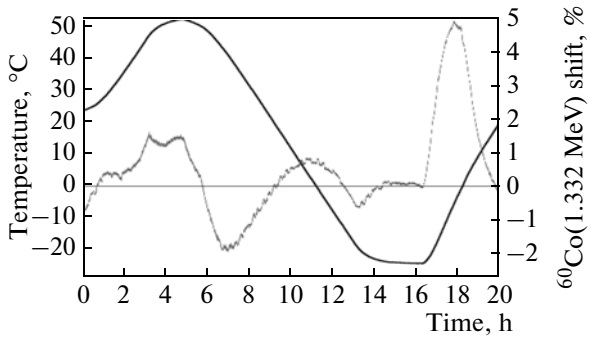

Fig. 8. Variation in the temperature of the crystal (heavy line, scale on the left) and the corrected ^{60}Co peak (1.332 MeV) shift (thin line, scale on the right) with time elapsed from the start of the measurements.

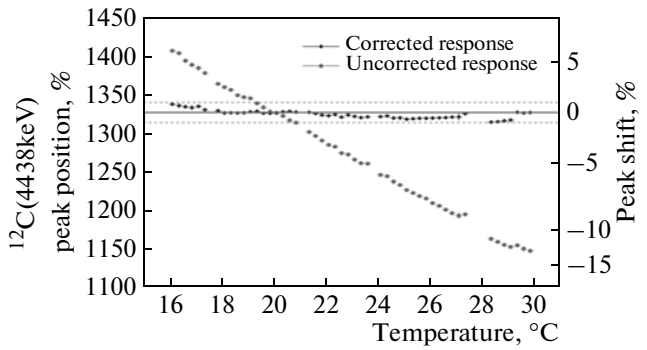

Fig. 9. Dependence of the absolute (scale on the left) and relative (scale on the right) positions of the ^{12}C (4438 keV) peak in the amplitude spectrum of the corrected and uncorrected gamma detector response on the temperature of the crystal.

tion algorithm was tested using a climate chamber with normalization to $T_0 = 20$°C. Figure 8 shows that the γ-detector response variations did not exceed 2% when the crystal was cooled from +55 to −20°C. The maximum deviation of 5% was observed at the beginning of the spontaneous warming up to room temperature when the chamber cooler was switched off.

The results of application of the software method of the gamma-detector response stabilization in the DVIN-1 portable inspection complex [3] are presented on Fig. 9. The temperature of the gamma detector rose from 16 to 30°C over 4 h of operation due to heat generation by the neutron generator and detecting electronics. The 14° change in the temperature of the crystal resulted in a 20% relative shift of the ^{12}C carbon peak (4438 keV) in the uncorrected spectrum, while the shift of this peak from the position at 20°C in the corrected data did not exceed ±1%.

CONCLUSIONS

The high γ-quanta detection efficiency, mechanical strength, and radiation resistance of BGO crystals motivated our choice of this scintillator for γ-detector systems intended for the detection and identification of concealed explosives and narcotics. The BGO-based gamma detector exhibits good response linearity. The typical energy resolution of such a detector equals 4.6% (if measured for the 4438 keV carbon line) at a time resolution of an α–γ coincidences detection system of 3.2 ns. The stability of the detector energy calibration in the temperature range from −20 to +50°C is ensured by proprietary software that introduces the temperature correction of the γ-detector response. This correction method is nowadays used in all explosives and narcotics detection systems produced at JINR and guarantees the energy calibration stability of about ±1%, which is sufficient for the reliable detection of explosives and narcotics in the operating temperature range.

ACKNOWLEDGMENTS

We would like to thank P.P. Reunov, T.O. Rudenko, A.I. Rudenko, and G.A. Kononenko for their help in constructing the γ-detectors.

REFERENCES

1. V. M. Bystritsky et al., Phys. Part. Nucl. Lett. **5**, 441–446 (2008).
2. V. M. Bystritsky et al., Phys. Part. Nucl. Lett. **6**, 505–510 (2009).
3. M. G. Sapozhnikov, Transp. Bezop. Tekhnol., No. 29, 120–121 (2012).
4. V. M. Bystritsky et al., Preprint JINR-E13-2006-36 (Joint Institute for Nuclear Research, Dubna, 2006).
5. Yu. K. Akimov, *Photonic Methods of Radiation Detection* (Joint Institute for Nuclear Research, Dubna, 2006) [in Russian].
6. M. Globus, B. Grinyov, and J. K. Kim, *Inorganic Scintillators for Modern and Traditional Applications* (Institute for Single Crystals, Kharkov, 2005).
7. Review of Russian radiometric and spectrometric systems that may be used in nuclear materials inspection and monitoring. http://www.vniia.ru/rgamo/literat/obzor/doc/obzorrus.pdf.
8. S. Normand et al., Nucl. Instrum. Methods Phys. Res., Sect. A **572**, 754–759 (2007).
9. J. Beringer et al. (Particle Data Group), Phys. Rev. D **86**, 010001 (2012).
10. B. Perot et al., Nucl. Instrum. Methods Phys. Res., Sect. B **261**, 295–298 (2007).
11. G. Perret et al., J. Phys.: Conf. Ser. **41**, 375–383 (2006).
12. M. Gierlik et al., IEEE Trans. Nucl. Sci. **53**, 1737–1743 (2006).
13. R. Sullivan, An advanced ESTCP PELAN system for surface and near-surface UXO discrimination.

http://www.dtic.mil/cgi-bin/GetTRDoc?AD=ADA512848.

14. C. Eleon et al., Nucl. Instrum. Methods Phys. Res., Sect. A **629**, 220–229 (2011).
15. Yu. A. Borovlev et al., J. Cryst. Growth **229**, 305–311 (2001).
16. Ya. V. Vasiliev et al., Nucl. Instrum. Methods Phys. Res., Sect. A **379**, 533–535 (1996).
17. Characteristics of bismuth orthogermanate $Bi_4Ge_3O_{12}$ (BGO) scintillation crystals. http://www.niic.nsc.ru/products/materials/bgo/.
18. Hamamatsu Photonics R6233-100 photomultiplier tube specifications. http://www.hamamatsu.com/us/en/R6233-100.html.
19. Analog Devices TMP36 low voltage temperature sensor data sheet. http://www.analog.com/static/imported-files/data_sheets/TMP35_36_37.pdf.
20. M. Bosteels and R. Weill, Nucl. Instrum. Methods Phys. Res., Sect. B **498**, 165–189 (2003).
21. P. C. Womble et al., in *Proceedings of SPIE Volume 4507: Hard X-Ray and Gamma-Ray Detector Physics III*, Ed. by R. B. James (SPIE, 2001), pp. 226–231.
22. S. A. Wender et al., Nucl. Instrum. Methods Phys. Res. **197**, 591–592 (1982).
23. Y. Karyotakis, in *Proceedings of the 1994 Beijing Calorimetry Symposium, Beijing, China, 1994*, Ed. by H. S. Chen (Institute of High Energy Physics, Beijing, 1995), pp. 27–35.
24. J. Isbert et al., Adv. Space Res. **42**, 437–441 (2008).

Translated by D. Safin